Synthesis and Characterization of the Organoindium Phosphides R_2InPPh_2 (R = *i*-Pr, CH_2Ph) and the Heterocubane $[MesInPMes]_4$

Bert Werner and Bernhard Neumüller*

Fachbereich Chemie der Universität Marburg, Hans-Meerwein-Straße, D-35032 Marburg, Germany

Received February 6, 1996[⊗]

The reaction of *i*-Pr_2InCl and $(PhCH_2)_2InCl$ with $LiPPh_2$ in Et_2O/THF or Et_2O/*n*-pentane gives the organoindium phosphides *i*-Pr_2InPPh_2 (**1**) and $(PhCH_2)_2InPPh_2$ (**2**), respectively. The tetrameric compound $[MesInPMes]_4$ (**3**) has been prepared by the treatment of $MesInCl_2$ with $MesPLi_2$ in Et_2O. **1**−**3** have been characterized by NMR, IR, and MS techniques as well as by X-ray diffraction. According to cryoscopic molecular weight determinations in benzene, **1** and **2** are present as a monomer−dimer equilibrium mixture, while **3** is tetrameric in solution. The X-ray analyses of **1** and **2** confirm the existence in the solid state of trimers in $[i\text{-}Pr_2InPPh_2]_3$ and $[(PhCH_2)_2InPPh_2]_3 \cdot OEt_2$ with distorted In_3P_3 six-membered rings in boat conformations. According to its structural characterization $[MesInPMes]_4 \cdot 4.5THF$ is a heterocubane with an In_4P_4 core shielded by the bulky organic groups.

Many of the recent developments in the chemistry of group 13−15 compounds have been induced by their possible use as single-source precursors for semiconducting materials.[1−3] In particular the formation of cyclic and cage compounds of Ga and In has been the focus of intensive research efforts.[4−16]

Both objectives require on the one hand a knowledge of the most effective synthetic procedures and on the other hand, an understanding of the thermodynamic and kinetic reasons for the formation and stabilization of the different ring and cage sizes in the gas phase, in solution, and in the solid state. Therefore, spectroscopic studies, mass spectral investigations, and X-ray structure determinations, combined with cryoscopic data, play important roles in research in this field.

One of the major problems in forming cages from starting compounds such as $RMCl_2$ (M = Al, Ga, In) and $R'PLi_2$ is the buildup of the cage in single-step reactions (eq 1). The stepwise generation of M−P bonds may lead

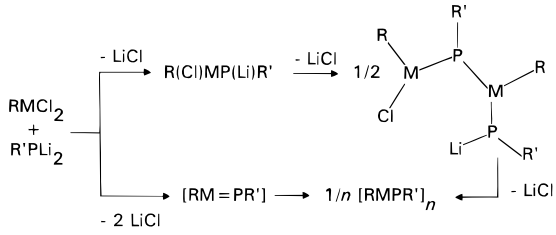

(1)

in the wrong direction, producing polymeric material. The intermediate formation of a molecule with an M=P double bond, which is a possible reaction pathway to M−P cages, was not observed. The well-known dilution principle favors the ring-closure reactions over polycondensation reactions. Heterocubanes such as $[i\text{-PrGaP}(t\text{-Bu})]_4$, $[(MesGa)_3\{GaP(H)(t\text{-Bu})\}\{P(t\text{-Bu})\}_4]$,[12] and $[(MesGa)_3\{GaP(H)Mes\}(PMes)_4]$[13] (Mes = 2,4,6-$Me_3C_6H_2$) can be isolated in an average yield of 30%. However, a total suppression of side reactions such as polycondensation is not possible. Therefore, the isolation of pure oligomers such as the heterocubanes depends on the availability of a suitable purification process: in particular, the purification by several steps of recrystallization.

In contrast to this, reactions with reactants possessing very bulky organic substituents such as adamantyl (Ad), 2,4,6-(*t*-$Bu)_3C_6H_2$ (Mes*), 2,4,6-(*i*-$Pr)_3C_6H_2$ (Trip), 2,4,6-$Ph_3C_6H_2$ (Mes**), and $SiPh_3$ give acceptable and often good yields of ring and cage compounds. Among these have been $[i\text{-BuAlPSiPh}_3]_4$, $[t\text{-BuGaPSiPh}_3]_4$,[4] $[Mes^{**}\text{-}GaP(C_6H_{11})]_3$,[5] $[(Trip)_3Ga_4(PAd)_4\{P(H)Ad\}]$,[6] $[t\text{-BuGaPMes*}]_2$,[7] and $[i\text{-PrInPSiPh}_3]_4$.[10] A variant of the metathesis reaction, the elimination of Me_3SiCl, gave in 86% yield the organometal-substituted heterocubane $[\{Cp(CO)_3Mo\}InPSiMe_3]_4$.[16]

Experimental Section

General Procedures. All experiments were carried out under an atmosphere of argon using Schlenk techniques. Purification and drying of the organic solvents were performed

[⊗] Abstract published in *Advance ACS Abstracts,* September 1, 1996.

(1) Cowley, A. H.; Jones, R. A. *Angew. Chem., Int. Ed. Engl.* **1989**, *28*, 1208.
(2) Cowley, A. H. *J. Organomet. Chem.* **1990**, *400*, 71.
(3) *Chemistry of Aluminium, Gallium, Indium and Thallium*, Downs, A. J., Ed.; Blackie Academic and Professionals: London, 1993.
(4) Cowley, A. H.; Jones, R. A.; Mardones, M. A.; Atwood, J. L.; Bott, S. G. *Angew. Chem., Int. Ed. Engl.* **1990**, *29*, 1409.
(5) Hope, H.; Pestana, D. C.; Power, P. P. *Angew. Chem., Int. Ed. Engl.* **1991**, *30*, 691.
(6) Waggoner, K. M.; Parkin, S.; Pestana, D. C.; Hope, H.; Power, P. P. *J. Am. Chem. Soc.* **1991**, *113*, 3597.
(7) Atwood, D. A.; Cowley, A. H.; Jones, R. A.; Mardones, M. A. *J. Am. Chem. Soc.* **1991**, *113*, 7050.
(8) Cowley, A. H.; Jones, R. A.; Mardones, M. A.; Atwood, J. L.; Bott, S. G. *Angew. Chem., Int. Ed. Engl.* **1991**, *30*, 1141.
(9) Power, M. B.; Barron, A. R. *Angew. Chem., Int. Ed. Engl.* **1991**, *30*, 1353.
(10) Atwood, D. A.; Cowley, A. H.; Jones, R. A.; Mardones, M. A. *J. Organomet. Chem.* **1993**, *449*, C1.
(11) Petrie, M. A.; Power, P. P. *Organometallics* **1993**, *12*, 1592.
(12) Niediek, K.; Neumüller, B. *Chem. Ber.* **1994**, *127*, 67.
(13) Niediek, K.; Neumüller, B. *Z. Anorg. Allg. Chem.* **1995**, *621*, 889.
(14) Belgardt, T.; Roesky, H. W.; Noltemeyer, M.; Schmidt, H.-G. *Angew. Chem., Int. Ed. Engl.* **1993**, *32*, 1056.
(15) Belgardt, T.; Waezsada, S. D.; Roesky, H. W.; Gornitzka, H.; Häming, L.; Stalke, D. *Inorg. Chem.* **1994**, *33*, 6247.
(16) App, U.; Merzweiler, K. Z. *Anorg. Allg. Chem.* **1995**, *621*, 1731.

S0276-7333(96)00077-5 CCC: $12.00

using standard methods.[17] *i*-Pr_2InCl,[18] $(PhCH_2)_2InCl$,[19,20] $MesInCl_2$,[21] $LiPPh_2$, and $MesPLi_2$[22] were prepared by following literature procedures.

The ^1H, ^{13}C, and ^{31}P NMR spectra were recorded on Bruker AC-300 (^1H, 300.134 MHz; ^{13}C, 75.469 MHz) and AM-400 spectrometers (^{31}P, 161.978 MHz). The standards were TMS (external; ^1H, ^{13}C) and aqueous 85% H_3PO_4 (external; ^{31}P) with δ 0.0 ppm. The IR spectra were obtained using a Bruker IFS-88 instrument (Nujol mulls, CsI disks for the range 4000−500 cm^{-1}, polyethylene disks for the range 500−100 cm^{-1}). For the EI mass spectra a Varian CH7a mass spectrometer (70 eV) was used. The melting points were measured with a Dr. Tottoli (Büchi) melting point apparatus in sealed capillaries under argon (values not corrected). The cryoscopic measurements were performed using a Normag molecular weight determination apparatus equipped with a Beckmann thermometer.

Synthesis of *i*-Pr_2InPPh_2 (1). A solution of 0.55 g (2.86 mmol) of $LiPPh_2$ in 15 mL of THF was added dropwise to 0.65 g (2.75 mmol) of *i*-Pr_2InCl in 15 mL of Et_2O at room temperature. The yellow reaction mixture was stirred overnight, and a small amount of LiCl precipitated. The solvent was removed under vacuum, and the yellow-green residue was treated with 15 mL of toluene. After filtration, the filtrate was evaporated to dryness. The solid was recrystallized from *n*-pentane, yielding colorless crystals (0.83 g, 78% yield based on *i*-Pr_2InCl; mp 124 °C dec). ^1H NMR (C_6D_6, ppm): 1.57 [m, 1 H, $HC(CH_3)_2$, monomer], 1.46 [d, $^3J(HH) = 7.60$ Hz, 6 H, $HC(CH_3)_2$, monomer, AB_6 spin system], 1.53 [m, 1 H, $HC(CH_3)_2$, dimer], 1.35 [d, $^3J(HH) = 7.55$ Hz, 6 H, $HC(CH_3)_2$, dimer, AB_6 spin system], 7.64−6.95 [m, phenyl *H*, monomer and dimer]. ^{13}C NMR (C_6D_6, ppm): 22.7 [$HC(CH_3)_2$, monomer], 23.4 [$HC(CH_3)_2$, dimer], 24.4 [$HC(CH_3)_2$, monomer], 25.3 [$HC(CH_3)_2$, dimer], 134.9 [$^1J(PC) = 18$ Hz, C^1, monomer], 134.1 [$^1J(PC) = 16.5$ Hz, C^1, dimer], 134.7 [$^2J(PC) = 7.5$ Hz, $C^{2/6}$, monomer], 134.5 [$^1J(PC) = 7.5$ Hz, $C^{2/6}$, dimer], 128.9 [$C^{3/5}$, dimer], 128.8 [$C^{3/5}$, monomer], 128.5 [C^4, dimer], 128.4 [C^4, monomer]. ^{31}P NMR (C_6D_6, ppm, 10 °C, 0.028 M) [δ (relative integral) species]: −27.3 (1) monomer, −48.5 (15.6) dimer; (25 °C, 0.028 M) −26.3 (1) monomer, −47.6 (2.8) dimer; (10 °C, 0.059 M) −27.3 (1) monomer, -48.5 (16.4) dimer; (25 °C, 0.059 M) −26.3 (1) monomer, -47.6 (5.6) dimer; (10 °C, 0.118 M) −26.3 (1) monomer, −47.5 (6.8) dimer. Cryscopic molecular weight, fw 386.18 [concentration (mol/L), wt, degree of association]: 0.028, 428, 1.1; 0.059, 505, 1.3; 0.118, 641, 1.7. IR (cm^{-1}): 502 (m, $\nu_{as}(InC_2)$), 476 (m, $\nu_s(InC_2)$), 364 (w, $\nu(In_3P_3)$). EI-MS [*m*/*z* (relative intensity) fragment]: 370 (1) $(M - Me)^+$, 228 (37) $(M - Me - Ph - C_5H_5)^+$, 115 (19) $(In)^+$, 108 (100) $(PPh)^+$. Anal. Calcd: C, 55.98; H, 6.26; P, 8.02. Found: C, 55.73; H, 6.23; P, 7.87.

Synthesis of $(PhCH_2)_2InPPh_2$ (2). A solution of 0.42 g (2.18 mmol) of $LiPPh_2$ in 7 mL of Et_2O was added dropwise to 0.67 g (2.01 mmol) of $(PhCH_2)_2InCl$ in 15 mL of *n*-pentane at room temperature. The colorless solution was stirred for 2 h, and the solvent was removed under vacuum. The solid residue was treated with 10 mL of toluene, and the solution was filtered. After removal of the toluene under vacuum a white powder remained, which was recrystallized from Et_2O, yielding colorless crystals (0.85 g, 86% yield based on $(PhCH_2)_2InCl$; mp 110 °C dec). ^1H NMR (0.03 mol/L, C_6D_6, ppm): 2.26 (s, 2 H, CH_2Ph), 6.5−7.4 (m, 10 H, phenyl *H*); (0.0145 mol/L): 2.34 (s, 1.0, CH_2Ph, monomer), 2.31 (s, 4.4, CH_2Ph, dimer). ^{13}C NMR (C_6D_6, ppm): 23.3 (CH_2Ph), 145.8 (C^1 benzyl), 128.8 ($C^{2/6}$ benzyl), 127.8 ($C^{3/5}$ benzyl), 122.6 (C^4 benzyl), 132.3 (C^1 PPh_2), 134.9 [$^2J(PC) = 7.8$ Hz, $C^{2/6}$ PPh_2], 129.4 [$^3J(PC) = 3.8$ Hz, $C^{3/5}$ PPh_2], 129.0 (C^4 PPh_2). ^{31}P NMR (25 °C, 0.03 mol/L, C_6D_6, ppm): −45.8; (25 °C, 0.0145 mol/L) −40.1 (1) monomer, −46.2 (4.5) dimer. Cryoscopic molecular weight, fw 482.27 [concentration (mol/L), wt, degree of association]: 0.0255, 926, 1.9; 0.0091, 853, 1.7. IR (cm^{-1}): 440 (m, $\nu(InC_2)$), 360 (m, $\nu(In_3P_3)$). EI-MS [*m*/*z* (relative intensity) fragment]: 292 (5) $(In_2P_2)^+$, $(In)^+$, 108 (73) $(PPh)^+$, 91 (54) $(PhCH_2)^+$, 77 (100) $(Ph)^+$. Anal. Calcd: C, 64.75; H, 5.02; P, 6.42. Found: C, 64.55; H, 5.11; P, 6,34.

Synthesis of $[MesInPMes]_4$ (3). Suspensions of 4.35 g (14.27 mmol) of $MesInCl_2$ in 40 mL of Et_2O and of 2.50 g (15.24 mmol) of $MesPLi_2$ in 40 mL of Et_2O were dropped simultaneously into 50 mL of Et_2O at −78 °C. The reaction mixture then was warmed to room temperature over 3 h and stirred for an additional 18 h. The solvent was removed under vacuum, and the orange residue was treated with 50 mL of toluene. After filtration, the toluene was removed under vacuum and the residue was treated with 40 mL of *n*-pentane. The suspension was filtered and the separated solid was washed with small portions of *n*-pentane and Et_2O until the solid was pale yellow. This residue was recrystallized from *n*-pentane/THF (0.79 g, 12% yield based on $MesInCl_2$; mp 174 °C dec). Suitable crystals of $[MesInPMes]_4$·4.5THF were obtained by slow recrystallization from *n*-pentane/THF over several weeks. ^1H NMR (C_6D_6, ppm): 1.89 [s, 3 H, CH_3-C^4(P)], 2.00 [s, 3 H, CH_3-C^4(In)], 2.13 [s, 6 H, CH_3-$C^{2/6}$(P)], 2.44 [s, 6 H, CH_3-$C^{2/6}$(In)], 6.56 [s, 2 H, *H*-$C^{3/5}$(In)], 6.67 [s, 2 H, *H*-$C^{3/5}$(P)]. ^{13}C NMR (C_6D_6, ppm): 20.7 [s, CH_3-C^4(P)], 21.2 [s, CH_3-C^4(In)], 26.1 [s, CH_3-$C^{2/6}$(In, P)], C^1(In) not observed, 144.2 [s, $C^{2/6}$(In)], 142.4 [s, C^4(P)], 138.2 [s, $C^{2/6}$(P)], 137.8 [s, C^1(P)], 136.2 [s, C^4(In)], 129.4 [s, $C^{3/5}$(P)], 128.3 [s, $C^{3/5}$(In)]. ^{31}P NMR (C_6D_6, ppm): −75.5. Cryscopic molecular weight, fw 1536.66 [concentration (mol/L), wt, degree of association]: 0.00253, 1526, 4.0 (based on a hypothetical monomer). IR (cm^{-1}): 548 (m, ν(InC)), 538 (m, ν(InC)), 388 (w, $\nu(In_4P_4)$). EI-MS [*m*/*z* (relative intensity) fragment]: 471 (2) $(In_3P_4 + 2H)^+$, 417 (3) $(InP_2Mes_2 + 2H)^+$, 353 (34) $(Mes_2In)^+$, 299 (22) $(P_2Mes_2 - H)^+$, 115 (55) $(In)^+$, 105 (100) $(PMes - 2Me)^+$. Anal. Calcd: C, 56.28; H, 5.77; P, 8.06. Found: C, 56.52; H, 5.78; P, 7.83.

X-ray Structure Determinations of $[1]_3$, $[2]_3$·OEt_2, and 3·4.5THF. The crystals were covered with a high-boiling paraffin oil and mounted on the top of a glass capillary under a flow of cold gaseous nitrogen. The orientation matrix and preliminary unit cell dimensions were determined from 25 reflections on a four-circle diffractometer with graphite-monochromated Mo Kα radiation ($\lambda = 71.073$ pm; Siemens P4). The final cell parameters were determined with 25 high-angle reflections.

The intensities have been corrected for Lorentz and polarization effects (for cell parameters and collecting of the intensities, see Table 1). The structures of $[\mathbf{1}]_3$ and **3**·4.5THF were solved by direct methods; the structure of $[\mathbf{2}]_3$·OEt_2 was solved by the Patterson method using the program SHELXTL-Plus.[23] The structures were refined against F^2 by full-matrix least squares with the program SHELXL-93.[24] The positions of the hydrogen atoms were calculated for ideal positions and refined with a common displacement parameter. The calculation of the bond lengths, bond angles, and U_{eq} values was performed using the program PLATON.[25] One *i*-Pr group in $[\mathbf{1}]_3$ is disordered and was refined in two positions (occupation factors: C121, 0.55; C122, 0.45). The THF molecules in **3**·4.5THF are disordered, one of them around a center of symmetry. The carbon atoms of the THF molecules have been refined with isotropic displacement parameters.

(17) Perrin, D. D.; Armarego, W. L. F.; Perrin, D. R. *Purification of Laboratory Chemicals*, 2nd ed.; Pergamon Press: Oxford, U.K., 1980.
(18) Neumüller, B. *Chem. Ber.* **1989**, *122*, 2283.
(19) Barron, A. R. *J. Chem. Soc., Dalton Trans.* **1989**, 1625.
(20) Neumüller, B. *Z. Anorg. Allg. Chem.* **1991**, *592*, 42.
(21) Leman, J. T.; Barron, A. R. *Organometallics* **1989**, *8*, 2214.
(22) Niediek, K.; Neumüller, B. *Z. Anorg. Allg. Chem.* **1993**, *619*, 885 and references cited therein.
(23) Sheldrick, G. M., SHELXTL-Plus, Release 4.2, for Siemens R3 Crystallographic Research Systems; Siemens Analytical X-ray Instruments, Inc., Madison, WI, 1990.
(24) Sheldrick, G. M. SHELXL-93; University of Göttingen, Göttingen, Germany, 1993.
(25) Spek, A. L. PLATON-94; University of Utrecht, Utrecht, The Netherlands, 1994.

Table 1. Crystallographic Data for Compounds [1]$_3$, [2]$_3$·OEt$_2$, and 3·4.5THF

	[**1**]$_3$	[**2**]$_3$·OEt$_2$	**3**·4.5THF
formula	$C_{54}H_{72}In_3P_3$	$C_{82}H_{82}In_3OP_3$	$C_{90}H_{124}In_4O_{4.5}P_4$
fw	1158.55	1520.93	1861.14
cryst size (mm)	0.1 × 0.65 × 0.65	0.4 × 0.4 × 0.35	0.32 × 0.2 × 0.17
a (pm)	4074.2(7)	1353.2(2)	1671.1(3)
b (pm)	1239.7(2)	1515.4(2)	1736.9(3)
c (pm)	2147.2(3)	1843.3(3)	1897.6(3)
α (deg)		77.67(1)	109.47(1)
β (deg)	92.06(1)	81.11(1)	100.46(1)
γ (deg)		89.65(1)	113.49(1)
V (10^6 pm^3)	10838(3)	3647(1)	4437(1)
space group	*C*2/*c*	$P\bar{1}$	$P\bar{1}$
No.[40]	15	2	2
Z	8	2	2
ρ_{calcd} (g/cm^3)	1.420	1.385	1.393
temp (K)	223	223	223
μ (cm^{-1})	13.9	10.3	11.5
2θ range (deg)	4−50	4−50	4−48
h,*k*,*l* values	$-1 \le h \le 46$, $-1 \le k \le 14$, $-25 \le l \le 25$	$-1 \le h \le 16$, $-17 \le k \le 17$, $-21 \le l \le 21$	$-1 \le h \le 18$, $-17 \le k \le 16$, $-21 \le l \le 21$
no. of rflns	11 459	14 567	14 833
no. of unique rflns	9524	12 790	13 260
no. of rflns with $F_o > 4\sigma(F_o)$ for R1	5087	8083	4621
no. of params	551	778	818
R_1[a]	0.0389	0.0351	0.0562
wR_2[b]	0.0714	0.0662	0.1239
weight factor *a*[c]	0.021	0.0267	0.0375

[a] $R_1 = \sum||F_o| - |F_c||/\sum|F_c|$. [b] $wR_2 = \{[\sum w(F_o^2 - F_c^2)^2]/[\sum w(F_o^2)^2]\}^{1/2}$. [c] $w = 1/[\sigma^2(F_o^2) + (aP)^2]$ and $P = [\max(F_o^2, 0) + 2F_c^2]/3$.

Selected bond lengths and angles of [**1**]$_3$, [**2**]$_3$·OEt$_2$, and **3**·4.5THF are listed in Table 2.

Results and Discussion

The diorganoindium phosphides **1** and **2** were synthesized by the reaction of *i*-Pr$_2$InCl and (PhCH$_2$)$_2$InCl, with LiPPh$_2$ in Et$_2$O at room temperature (eq 2). **1** and

$$R_2InCl + LiPPh_2 \xrightarrow{Et_2O;\ room\ temp} R_2InPPh_2 + LiCl \quad (2)$$

1: R = *i*-Pr
2: R = CH$_2$Ph

2 both are air-sensitive and show a pronounced sensitivity toward light in solution. The colorless crystals of [**1**]$_3$ and [**2**]$_3$·OEt$_2$ are photostable.

In the preparation of **3** both reactants were suspended in Et$_2$O and added slowly and simultaneously to cold Et$_2$O (eq 3).

$$MesInCl_2 + MesPLi_2 \xrightarrow{Et_2O} {}^1/_4[MesInPMes]_4 + 2LiCl \quad (3)$$

3

Solutions of **1**−**3** in C$_6$D$_6$ give quite different NMR spectra. The ^{31}P NMR spectra of **3** show a singlet, independent of concentration and temperature, at −75.5 ppm. In solutions of **2** in C$_6$D$_6$ at concentrations higher than 0.03 mol/L only one signal at −45.8 ppm is observable. Diluted samples (a typical concentration is 7 mg of **2** in 1 mL of solvent) give two resonances at −40.1 and −46.2 ppm. In the ^{31}P NMR spectrum of **1** two signals are observed at −26.6 and −47.8 ppm. This is in good agreement with investigations of Beachley et al. concerning the monomer−dimer equilibrium in solutions of [(Me$_3$SiCH$_2$)$_2$InPPh$_2$]$_2$[26] and [(Me$_3$CCH$_2$)$_2$InPPh$_2$]$_3$.[27] The results of the cryoscopic measurements seen in the context of the ^{31}P NMR spectra for **1** at variable temperature agree with the data reported in the literature (see Experimental Section). On the basis of these facts, the resonance at −26.6 ppm can be assigned to the monomer species, while the line at −47.8 ppm is due to the dimer. However, this does not agree with our observations that an increase of Lewis-acidic metal centers at a phosphorus atom leads to a downfield shift of the resonance.[12,13] According to these findings the assignment of the signals to the species in solution should be the opposite. One explanation which can be put forward to resolve this conflict is the coordination number (CN) of the phosphorus atom. The phosphorus atom exhibits a CN of 3 in the monomer, while the CN in the dimer is 4. This may cause an unexpected effect. The ^{31}P NMR signal at −40.1 ppm increases with the decrease of the concentration of **2** in C$_6$D$_6$. According to the cryoscopic data the degree of association decreases at the same time. An estimation of the ^{31}P NMR signals and a comparison with the measured degree of association is in good agreement (use of a transient delay time leads not to a significant modification of the integral ratio). Surprisingly, the temperature dependence of **2** is the opposite of the behavior measured for **1**. The singlet at −40.1 ppm assigned to the monomer increases in intensity during cooling. The monomer:dimer ratio changes reversibly from 1:4.5 (60 °C) to 1.3:1 (−60 °C). We do not know whether solvent−indium interactions or intermolecular CH$_2$Ph-In contacts[20] are responsible for this behavior at this time. For **3**, the ^{31}P NMR signal and the degree of association as determined by cryoscopy are in good agreement.

(26) Beachley, O. T., Jr.; Kopasz, J. P.; Zhang, H.; Hunter, W. E.; Atwood, J. L. *J. Organomet. Chem.* **1987**, *325*, 69.
(27) Banks, M. A.; Beachley, O. T., Jr.; Buttrey, L. A.; Churchill, M. R.; Fettinger, J. C. *Organometallics* **1991**, *10*, 1901.

Table 2. Selected Bond Lengths (pm) and Angles (deg) for [1]$_3$, [2]$_3$·OEt$_2$, 3·4.5THF

	Compound [**1**]$_3$		
In1−P1	263.5(2)	In1−P3	263.0(2)
In2−P1	265.0(1)	In2−P2	266.4(2)
In3−P2	265.3(2)	In3−P3	265.3(2)
In1−C1	218.9(6)	In1−C2	221.1(6)
In2−C3	220.6(6)	In2−C4	221.1(6)
In3−C5	218.5(6)	In2−C6	219.0(6)
P1−In1−P3	101.29(4)	P1−In2−P2	99.78(5)
P2−In3−P3	97.58(5)	In1−P1−In2	125.77(5)
In2−P2−In3	131.23(5)	In1−P3−In3	127.99(5)
C1−In1−C2	119.5(3)	C3−In2−C4	123.5(3)
C5−In3−C6	119.1(3)		
	Compound [**2**]$_3$·OEt$_2$		
In1−P1	262.5(1)	In1−P3	259.4(1)
In2−P1	263.0(1)	In2−P2	261.1(1)
In3−P2	263.8(1)	In3−P3	261.6(1)
In1−C1	220.3(4)	In1−C2	218.6(5)
In2−C3	218.5(4)	In2−C4	219.2(4)
In3−C5	219.1(4)	In3−C6	219.0(4)
P1−In1−P3	100.99(4)	P1−In2−P2	98.83(4)
P2−In3−P3	107.47(4)	In1−P1−In2	131.34(5)
In2−P2−In3	125.14(4)	In1−P3−In3	116.54(4)
C1−In1−C2	114.6(2)	C3−In2−C4	114.6(2)
C5−In3−C6	124.3(2)		
	Compound **3**·4.5THF		
In1−P1	261.2(3)	In1−P2	258.7(3)
In1−P4	261.4(3)	In2−P1	258.2(3)
In2−P2	262.3(3)	In2−P3	260.0(3)
In3−P1	260.8(3)	In3−P3	258.6(3)
In3−P4	262.0(3)	In1−C1	221(1)
In2−C2	214(1)	In3−C3	217(1)
In4−C4	214(1)		
P1−In1−P2	87.8(1)	P1−In1−P4	88.8(1)
P2−In1−P4	87.9(1)	P1−In2−P2	87.7(1)
P1−In2−P3	87.2(1)	P2−In2−P3	88.1(1)
P1−In3−P3	87.0(1)	P1−In3−P4	88.7(1)
P3−In3−P4	88.0(1)	P2−In4−P3	87.9(1)
P2−In4−P4	87.9(1)	P3−In4−P4	88.2(1)
In1−P1−In2	92.4(1)	In1−P1−In3	91.3(1)
In2−P1−In3	92.8(1)	In1−P2−In2	92.1(1)
In1−P2−In4	92.0(1)	In2−P2−In4	91.6(1)
In2−P3−In3	92.9(1)	In2−P3−In4	92.2(1)
In3−P3−In4	91.9(1)	In1−P4−In3	91.0(1)
In1−P4−In4	92.2(1)	In3−P4−In4	91.8(1)
P−In−C[a]	126.6	In−P−C[a]	123.8

[a] Average value.

Only one set of signals could be observed in the ^{1}H and ^{13}C NMR spectra of **3**. The ^{1}H and ^{13}C NMR spectra of **1** and **2** (at high dilution) exhibit two sets of signals, confirming the monomer-dimer equilibrium. The AB$_6$ spin system found for the *i*-Pr groups in **1** are especially characteristic (1.53 ppm *H*C(CH$_3$)$_2$, 1.35 ppm HC(C*H*$_3$)$_2$, dimer; 1.57 ppm *H*C(CH$_3$)$_2$, 1.46 ppm HC(C*H*$_3$)$_2$, monomer).[18,28,29]

The IR spectra exhibit asymmetric and symmetric stretching vibrations at 502 and 476 cm^{-1}.[18,30,31] The value for the vibration ν(InC$_2$) in **2** is 440 cm^{-1}.[20] The two absorptions at 548 and 538 cm^{-1} in **3** have been assigned to the In−C stretching vibrations,[32] although these bands have a strong Mes-ring component.[33] Of great interest are the In$_3$P$_3$ (**1**, **2**) and In$_4$P$_4$ (**3**) skeletal vibrations. It was shown for [Me$_2$GaP(SiMe$_3$)$_2$]$_2$ that all ring vibrations are mixed with exocyclic ring atom−ligand components.[34] We assume that the bands at 364, 235 (**1**), 360, 208 (**2**), and 388 cm^{-1} (**3**) have a strong In−P skeleton character.

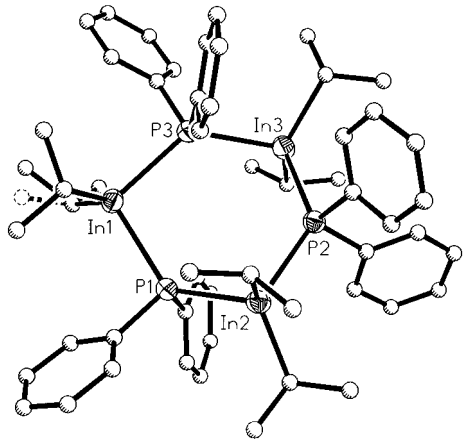

Figure 1. Molecule [**1**]$_3$ with disorder behavior of a *i*-Pr group. In and P atoms are shown at the 50% probability level; the C atoms are drawn as balls for clarity.

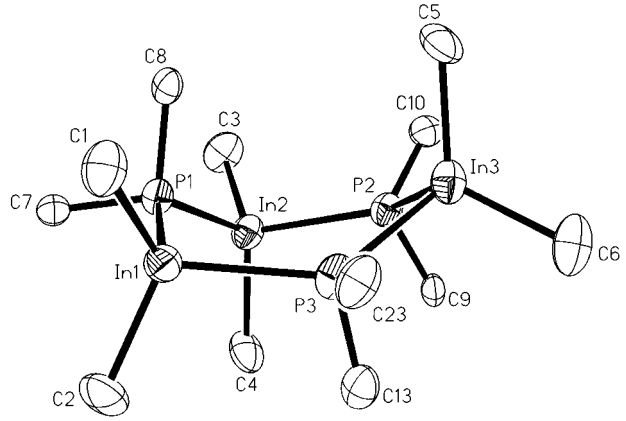

Figure 2. Distorted-boat form of the In$_3$P$_3$ backbone of [**1**]$_3$. The organic substituents are reduced to *ipso* C atoms or methine C atoms (50% ellipsoids).

Only fragments of [**1**]$_3$, [**2**]$_3$, and **3** could be found in the EI mass spectra. While **1** gives a signal at *m*/*z* 370 ((M−Me)$^+$), the mass spectra of **2** and **3** show only fragments of their M−P skeleton at *m*/*z* 292 (In$_2$P$_2$) and *m*/*z* 471 ((In$_3$P$_3$ + 2H)$^+$).

The solid-state structures of [**1**]$_3$ and [**2**]$_3$·OEt$_2$ consist of six-membered In−P rings in a distorted-boat form. Figure 1 shows a molecule of [**1**]$_3$, Figure 2 gives the In$_3$P$_3$ framework of [**1**]$_3$. The graphical representation of [**2**]$_3$ in [**2**]$_3$·OEt$_2$ is depicted in Figure 3 , while Figure 4 displays the In$_3$P$_3$ skeleton of [**2**]$_3$. The In−P distances in [**1**]$_3$ (265 pm, average) and [**2**]$_3$ (262 pm, average) are typical for cyclic organometallic indium phosphides (see Table 3).[10,16,26,27,35−38] There is no obvious correlation between the In−P interatomic distances and the ring sizes. However, the bulk of the ligands and the number

(28) Neumüller, B. *Z. Naturforsch.* **1990**, *45B*, 1559.
(29) Neumüller, B. *Z. Naturforsch.* **1991**, *46B*, 753.
(30) Weidlein, J.; Müller, U.; Dehnicke, K. *Schwingungsfrequenzen I*; Thieme Verlag: Stuttgart, Germany, 1988.
(31) Schloz, G.; Weidlein, J. *Z. Anorg. Allg. Chem.* **1995**, *621*, 747.
(32) Neumüller, B.; Gahlmann, F. *J. Organomet. Chem.* **1991**, *414*, 271.
(33) Kainz, B.; Schmidt, A. *Spectrochim. Acta* **1990**, *46A*, 1361.
(34) Wiedmann, D.; Hausen, H.-D.; Weidlein, J. *Z. Anorg. Allg. Chem.* **1995**, *621*, 1351.
(35) Burns, J. A.; Dillingham, M. D. B.; Byers Hill, J.; Gripper, K. D.; Pennington, W. T.; Robinson, G. H. *Organometallics* **1994**, *13*, 1514.
(36) Beachley, O. T., Jr.; Maloney, J. D.; Banks, M. A.; Rogers, R. D. *Organometallics* **1995**, *14*, 3448 and references cited therein.
(37) Dembrowski, U.; Roesky, H. W.; Pohl, E.; Herbst-Irmer, R.; Stalke, D.; Sheldrick, G. M. *Z. Anorg. Allg. Chem.* **1992**, *611*, 92.
(38) Theopold, K. H.; Douglas, T. *Inorg. Chem.* **1991**, *30*, 594.

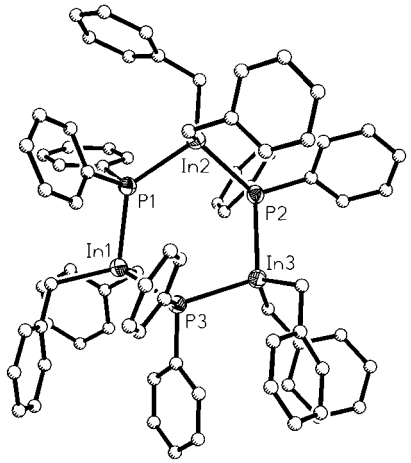

Figure 3. Molecule $[\mathbf{2}]_3$ of $[\mathbf{2}]_3 \cdot OEt_2$ In and P atoms are shown at the 50% probability level; the C atoms are drawn as balls for clarity.

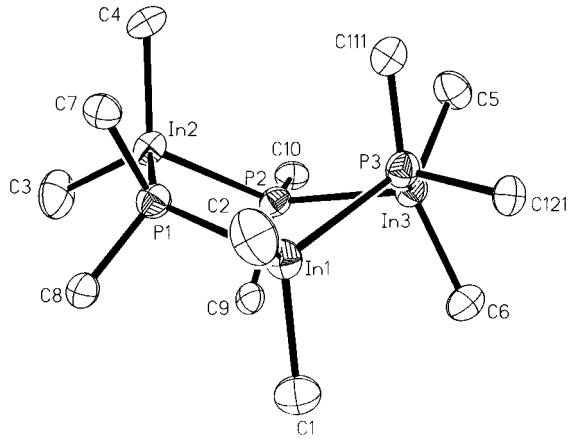

Figure 4. Distorted-boat form of the In_3P_3 backbone of $[\mathbf{2}]_3$. The organic substituents are reduced to *ipso* C atoms or methylene C atoms (50% ellipsoids).

Table 3. In−P Bond Lengths for Selected Indium−Phosphorus Compounds

compd	In−P (pm)	ref
$[\mathbf{1}]_3$	263.0(2)−266.4(2)	*a*
$[\mathbf{2}]_3 \cdot OEt_2$	259.4(1)−263.8(1)	*a*
3·4.5THF	258.2(3)−262.3(3)	*a*
$[i\text{-PrInPSiPh}_3]_4$	258.2(4)−260.3(4)	10
$[Cp(CO)_3MoInPSiMe_3]_4$	256.9(3)−263.2(3)	16
$[(Me_3CCH_2)_2InPPh_2]_3$	267.7(1), 269.9(2)	27
$[Me_2InPPh_2]_3$	259.3(1)−263.3(2)	35
$[(Me_3CCH_2)_2InP(H)C_6H_{11}]_3$	261.3(3)−265.9(2)	36
$[(Me_3SiCH_2)_2InPPh_2]_2$	263.2(2)−266.4(2)	26
$[(Me_3CCH_2)_2InPEt_2]_2$	262.3(2), 264.1(2)	36
$[(Me_3SiCH_2)_2InP(H)Ad]_2$	264.2(1), 267.6(1)	37
$[(C_5Me_5)(Cl)InP(SiMe_3)_2]_2$	259.4(1), 264.8(2)	38
$[Cl(Me_3SiCH_2)InP(SiMe_3)_2]_2$	259.1(1), 259.5(2)	41
$[Me(Me_3SiCH_2)InP(SiMe_3)_2]_2$	263.2(2), 263.8(1)	41

[a] This work.

of electronegative substituents seem to influence the metal−phosphorus distances. The neopentyl-substituted $[(Me_3CCH_2)_2InPPh_2]_3$ exhibits values of 267.7(1) and 269.9(2) pm.[27] Despite the fact that the dimer $[(C_5Me_5)(Cl)InP(SiMe_3)_2]_2$ contains the bulky ligand C_5Me_5, the In−P distances are 259.4(1) and 264.8(2) pm, probably due to the presence of chlorine atoms.[38] The trimeric molecules $[(Me_3CCH_2)_2InPPh_2]_3$,[27] $[Me_2InPPh_2]_3$[35] and $[(Me_3CCH_2)_2InP(H)C_6H_{11}]$,[36] related to $[\mathbf{1}]_3$ and $[\mathbf{2}]_3 \cdot OEt_2$, possess a chair form for the In_3P_3 backbone in the first two compounds and a twisted-boat

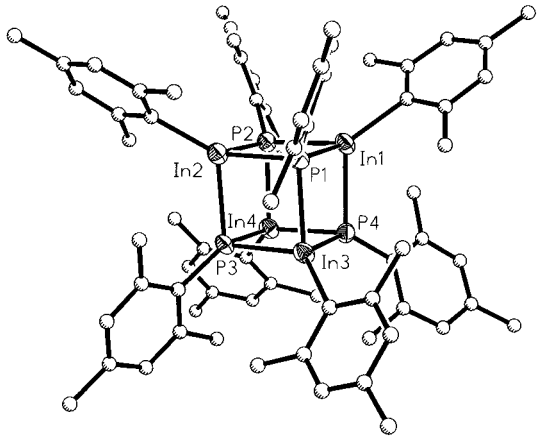

Figure 5. Heterocubane **3** from **3**·4.5THF. In and P atoms are shown at the 50% probability level; the C atoms are drawn as balls for clarity.

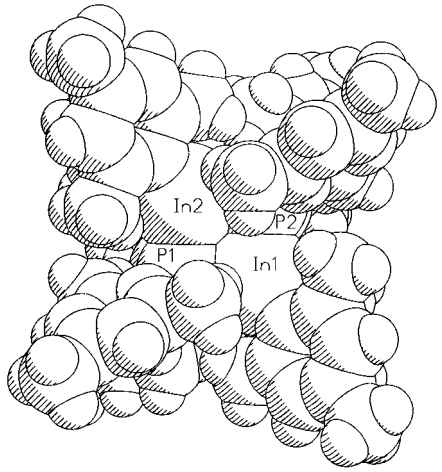

Figure 6. Space-filling model of **3**: view of one of the cube faces.

form in the last compound. However, both conformations, chair and boat, lead to P−In−P angles of approximately 100° and In−P−In angles of about 120°. It is remarkable that the compounds exhibiting boat conformations show one large In−P−In angle ($[\mathbf{1}]_3$, In2−P2−In3 = 131.23(5)°; $[\mathbf{2}]_3$, In1−P1−In2 = 131.34(5)°; $[(Me_3CCH_2)_2InP(H)C_6H_{11}]$, In2−P2−In3 = 132.18(8)). This can be explained as a consequence of the ring strain. A quite similar situation was found for Ga−P six-membered rings (Ga and P atoms possess CN 4).[39]

A CN of 4 for all cage atoms is also realized in the heterocubane molecule of **3**·4.5THF (Figure 5), although the presence of three P atoms around each In atom causes a slight shortening of the In−P bonds. The average value of 260.4 pm is in good agreement with measured In−P bond lengths in the heterocubanes $[i\text{-PrInPSiPh}_3]_4$[10] and $[Cp(CO)_3MoInPSiMe_3]_4$.[16] All P−In−P angles in **3** are smaller than 90° (average 88.0°), while the In−P−In angles are larger than 90° (average 92.0°). A common rule for this observation in

(39) See e.g.: (a) Cowley, A. H.; Harris, P. R.; Jones, R. A.; Nunn, C. M. *Organometallics* **1991**, *10*, 652. (b) Cowley, A. H.; Jones, R. A.; Mardones, M. A.; Nunn, C. M. *Organometallics* **1991**, *10*, 1635. (c) Elms, F. M.; Koutsantonis, G. A.; Raston, C. L. *J. Chem. Soc., Chem. Commun.* **1995**, 1669.

(40) *International Tables for Crystallography*, 2nd ed.; Kluwer Academic: Dordrecht, The Netherlands, 1989; Vol. A.

(41) Wells, R. L.; McPhail, A. T.; Jones, L. J., III; Self, M. F. *J. Organomet. Chem.* **1993**, *449*, 85.

M_4P_4 cages could not be found. Only in $[i\text{-PrInPSiPh}_3]_4$ has this special deformation been observed. $[i\text{-BuAlPSiPh}_3]_4$[4] exhibits the opposite architecture of the cube corners. In $[i\text{-PrGaP}(t\text{-Bu})]_4$[12] and $[Cp(CO)_3MoInPSiMe_3]_4$ as well as in molecules with strongly distorted M_4P_4 cages such as $[(MesGa)_3\{GaP(H)Mes\}(PMes)_4]$,[13] no pattern for the size of the P−In−P and the In-P-In angles, respectively, could be detected.

The space-filling model in Figure 6 shows that an evasion of the mesityl substituents is realized by the torsion of two aryl planes of direct neighbors. Thus, angles between 47 and 84° are formed.

Acknowledgment. This work was supported by the Deutsche Forschungsgemeinschaft and the Fonds der Chemischen Industrie.

Supporting Information Available: Tables of crystal data, atomic coordinates, bond lengths and angles, and isotropic or anisotropic displacement parameters for all atoms in $[\mathbf{1}]_3$, $[\mathbf{2}]_3\cdot OEt_2$, and $\mathbf{3}\cdot 4.5THF$ and text giving complete mass and IR spectral data (40 pages). Ordering information is given on any current masthead page.

OM960077P